

ON THE DUST TORI IN PALOMAR-GREEN QUASARS

XINWU CAO

Shanghai Astronomical Observatory, Chinese Academy of Sciences, 80 Nandan Road, Shanghai, 200030, China
 Email: cxw@shao.ac.cn

(Received 2004 July 4; accepted 2004 August 20)

Draft version October 10, 2018

ABSTRACT

The dust clouds in the torus of the quasar are irradiated by the central source, and the clouds at the inner radius of the torus re-radiate mostly in the near-infrared (NIR) wavebands. The ratio of the near-infrared luminosity to the bolometric luminosity $L_{\text{NIR}}/L_{\text{bol}}$ can therefore reflect the torus geometry to some extent. We find a significant correlation between the ratio of the near-infrared luminosity to the bolometric luminosity $L_{\text{NIR}}/L_{\text{bol}}$ and the central black hole mass M_{bh} for the Palomar-Green (PG) quasars, whereas no correlation is found between the Eddington ratio $L_{\text{bol}}/L_{\text{Edd}}$ and the ratio $L_{\text{NIR}}/L_{\text{bol}}$. Similar correlations are found for the mid-infrared and far-infrared cases. It may imply that the torus geometry, i.e., the solid angle subtended by the dust torus as seen from the central source, does not evolve with the accretion rate. The correlation of the solid angle subtended by the torus with the central black hole mass M_{bh} implies that the formation of the dust torus is likely regulated by the central black hole mass. We find that the torus thickness H increases with quasar bolometric luminosities, which is different with the constant torus thickness H with luminosity assumed in the receding torus model. The average relative thickness H/R of the tori in the PG quasars derived from the ratios of the infrared to bolometric luminosities is ~ 0.9 . The further IR observations on a larger quasar sample including more fainter quasars by the Spitzer Space Telescope will help understand the physics of the dust tori in quasars.

Subject headings: galaxies: active—quasars: general—accretion, accretion disks—black hole physics

1. INTRODUCTION

The putative dust torus is an important ingredient of the unification model for active galactic nuclei (AGNs) (Antonucci 1993). A type 1 AGN spectrum is yielded if the broad-line region (BLR) is directly viewed through the hole of the face-on dust torus, while the BLR is obscured by the torus seen edge-on that leads to a type 2 AGN spectrum. This model can successfully unify Seyfert 1 and Seyfert 2 galaxies; radio quasars and radio galaxies, etc (e.g., Antonucci & Miller, 1985; Miller & Goodrich 1990; Tran 1995; Barthel 1989), which is supported by a variety of observational features of AGNs (e.g., Lawrence 1991; Hill, Goodrich, & Depoy, 1996).

The dust torus is irradiated by the central engine of the AGN, and the dust cannot survive inside a critical radius at which the temperature is so high that the dust begins to sublimate. The temperature of the dust clouds at the inner edge of the torus is close to the sublimation temperature. The irradiated dust produces thermal emission mostly at the NIR wavelength. The decomposition of spectral energy distributions of AGNs suggested that the NIR continuum emission ($\gtrsim 2\mu\text{m}$) from Seyfert galaxies is dominated by thermal radiation from the hot dust surrounding the central engine (e.g., Kobayashi et al. 1993). The analysis on the infrared emission data of 64 Palomar-Green (PG) quasars favors the dust being heated by the central engines of AGNs (Haas et al. 2003). The inner radius of the dust torus is assumed to be roughly at the dust evaporation radius $R(T_{\text{evap}}) \simeq 0.06(L_{\text{bol}}/10^{38}\text{W})^{1/2}$ pc (Netzer & Laor 1996; Hill, Goodrich, & Depoy 1996). The intense monitoring observations were carried out on the Seyfert 1 galaxy NGC4151, and a lag time of 48^{+2}_3 days between the V and K light curves was measured. The inner radius of the dust torus in NGC4151 is ~ 0.04 pc corresponding to this measured time lag. For this source, the predicted evaporation radius $R(T_{\text{evap}}) \simeq 0.015$ pc

(Netzer & Laor, 1996; $L_{\text{bol}} \simeq 6.5 \times 10^{36}$ W, given by Kaspi et al., 2000), which is roughly consistent with the inner radius of the dust torus ~ 0.04 pc measured by thermal dust reverberation method (Minezaki et al. 2004). If the radio quasars and galaxies are intrinsically same and can be unified by their different orientations, the relative thickness of the torus $H/R \sim 2-3$ is estimated from the fraction of quasars in the 3CR sample (Hill, Goodrich, & Depoy 1996).

If the relative thickness H/R of the torus is around unity, the random velocities should be $\gtrsim 100\text{km s}^{-1}$ for the matter in the tori at sub-parsec scales, because the dust torus is required to be in dynamical equilibrium. If this motion is thermal, the corresponding temperature ($\sim 10^6$ K) is too high for dust to survive. It is therefore suggested that the cold dust is in the clouds moving at the random velocities $\gtrsim 100\text{km s}^{-1}$ (Krolik & Begelman 1988). The origin of such dust tori in AGNs is still a mystery, though Zier & Biermann (2001, 2002) suggested that the merger of binary black holes may lead the distribution of the surrounding matters to be a torus-like structure. In this paper, we perform statistic analysis on the properties of the dust tori in PG quasars. The cosmological parameters $\Omega_{\text{M}} = 0.3$, $\Omega_{\Lambda} = 0.7$, and $H_0 = 70 \text{ km s}^{-1} \text{ Mpc}^{-1}$ have been adopted in this work.

2. BLACK HOLE MASS

Kaspi et al. (2000) derived an empirical relation between the BLR size and optical continuum luminosity for a sample of Seyfert 1 galaxies and quasars using the cosmological parameters $H_0 = 75 \text{ km s}^{-1} \text{ Mpc}^{-1}$ and $q_0 = 0.5$, in which the sizes of BLRs are measured with the reverberation mapping method (Peterson 1993). The relation

$$R_{\text{BLR}} = (26.4 \pm 3.0) \left[\frac{\lambda L_{\lambda}(5100)}{10^{44} \text{ergs s}^{-1}} \right]^{0.610 \pm 0.10} \text{ lt-days} \quad (1)$$

is derived by McLure & Jarvis (2002) for the same sample,

but the cosmological parameters used are same as this work: $\Omega_M = 0.3$, $\Omega_\Lambda = 0.7$, and $H_0 = 70 \text{ km s}^{-1} \text{ Mpc}^{-1}$.

The central black hole masses M_{bh} can be estimated from the velocities v_{BLR} of the clouds in the BLRs

$$M_{\text{bh}} = \frac{v_{\text{BLR}}^2 R_{\text{BLR}}}{G}, \quad (2)$$

where the motions of the clouds are assumed to be virialized and isotropic. The velocities of the clouds in BLRs v_{BLR} are derived from the width of the broad emission lines. For most quasars, the BLR sizes have not been measured by the reverberation mapping method, and the empirical relation (1) is instead used to estimate the BLR sizes. The central black hole masses of quasars have been estimated from their broad-line widths and optical continuum luminosity (e.g., Laor, 2000; McLure & Dunlop 2001; Cao & Jiang 2002). For normal bright quasars, the bolometric luminosity can be estimated from their optical luminosity $L_{\lambda, \text{opt}}$ at 5100 Å by (Kaspi et al. 2000)

$$L_{\text{bol}} \simeq 9\lambda L_{\lambda, \text{opt}}. \quad (3)$$

Assuming a constant accretion efficiency for all quasars, we have the conventional defined dimensionless accretion rate

$$\dot{m} = \frac{L_{\text{bol}}}{L_{\text{Edd}}}. \quad (4)$$

3. TORUS GEOMETRY

The dust clouds at the inner edge of the torus irradiated by the AGN central engine produce thermal emission mostly in the NIR waveband (e.g., Kobayashi et al., 1993), so the NIR luminosity of the dust torus is estimated by

$$L_{\text{NIR}} \simeq \frac{\Delta\Omega_{\text{torus}}(R_{\text{in}})}{4\pi} f_{\text{in}} L_{\text{bol}}, \quad (5)$$

where L_{bol} is the bolometric luminosity of the AGN, $\Delta\Omega_{\text{torus}}$ is the solid angle subtended by the dust torus as seen from the central source at the inner radius R_{in} of the torus, and the factor f_{in} describes the covering factor of the clouds at the inner radius of the torus and the uncertainties. The uncertainties arising from the NIR emission contributed by the central continuum emission of the AGN and starbursts in the AGN host galaxy may not be large, because this emission can be neglected compared with the NIR emission from the tori in most PG quasars (Haas et al. 2003). If the contribution in the NIR waveband from stars in the host galaxy can be neglected compared with that from the torus, the factor f_{in} describes the covering factor. Thus, we can infer the dust torus geometry from the NIR and bolometric luminosities of AGNs,

$$\Delta\Omega_{\text{torus}}(R_{\text{in}}) = 4\pi f_{\text{in}}^{-1} \frac{L_{\text{NIR}}}{L_{\text{bol}}}, \quad (6)$$

if the covering factor of the dust clouds at the inner edge of the torus is known. If we assume all the IR emission of quasars is from the dust torus irradiated by the AGNs, we can estimate the solid angle subtended by the whole dust torus by

$$\Delta\Omega_{\text{torus}}^{\text{max}} = 4\pi \frac{L_{\text{IR}}}{L_{\text{bol}}}, \quad (7)$$

where the covering factor $f = 1$ is adopted, because the putative torus is required to be able to obscure the nuclear emission while it is seen edge-on (Antonucci 1993). If the torus is subtended at a constant solid angle with radius (i.e., cone-like

structure), the covering factor f_{in} at the inner radius R_{in} can be estimated by

$$f_{\text{in}} \simeq \frac{L_{\text{NIR}}}{L_{\text{IR}}}. \quad (8)$$

The solid angle estimated from Eq. (7) is an upper limit for some sources of which the IR emission from the host galaxies is important compared with that from the dust tori.

The solid angle subtended by the torus $\Delta\Omega_{\text{torus}}$ is

$$\Delta\Omega_{\text{torus}} = \frac{4\pi H/R}{(4 + H^2/R^2)^{1/2}}, \quad (9)$$

where H is the thickness of the torus. For the case of $H/R \lesssim 1$, Equation (9) can be approximated as

$$\Delta\Omega_{\text{torus}} \simeq \frac{2\pi H}{R}. \quad (10)$$

Combining the relations (6) and (9), we can roughly estimate the torus thickness at its inner edge by

$$H(R_{\text{in}}) = \frac{2f_{\text{in}}^{-1} R_{\text{in}} (L_{\text{NIR}}/L_{\text{bol}})}{[1 - f_{\text{in}}^{-2} (L_{\text{NIR}}/L_{\text{bol}})^2]^{1/2}} \text{ pc}, \quad (11)$$

where the inner radius R_{in} of the torus is given by $R_{\text{in}} \simeq 0.06(L_{\text{bol}}/10^{38} \text{ W})^{1/2} \text{ pc}$ (Netzer & Laor 1996; Hill, Goodrich, & Depoy 1996).

4. SAMPLE

Haas et al. (2003) provided a sample of 64 PG quasars with infrared spectral energy distributions (3–150 μm) observed by the ISO. The PG quasars have high infrared detection rate of more than 80 per cent. As discussed in Sect. 2, the central black hole masses in quasars can be estimated from their broad-line widths of $\text{H}\beta$ and optical continuum luminosities $\lambda L_\lambda(5100)$. The full widths at half maximum (FWHM) of broad-line $\text{H}\beta$ for 51 sources in this sample are available in Boroson & Green (1992). For the remainder, they are at relatively high redshifts ($z \gtrsim 1$). We search the literature and find $\text{FWHM}(\text{H}\beta) = 5100 \text{ km s}^{-1}$ for 0044+030 (Brotherton 1996); and $\text{FWHM}(\text{H}\beta) = 9601 \text{ km s}^{-1}$, 4613 km s^{-1} for 1634+706 and 1718+481, respectively (Shields et al. 2003). It leads to a sample of 54 quasars with estimated black hole masses, which includes 41 radio-quiet quasars and 13 radio-loud quasars (4 flat-spectrum and 9 steep-spectrum radio quasars). There are ten sources with $\text{FWHM}(\text{H}\beta) < 2000 \text{ km s}^{-1}$ in this sample (hereafter we refer to those quasars with $\text{FWHM}(\text{H}\beta) \geq 2000 \text{ km s}^{-1}$ as broad-line(BL) quasars).

5. RESULTS

We estimate the central black hole masses of these PG quasars using their broad-line widths of $\text{H}\beta$ and optical continuum luminosities as described in Sect. 2. The NIR luminosities L_{NIR} of the PG quasars in the waveband of 3–10 μm given by Haas et al. (2003) are used in this work to explore the properties of the tori at their inner radii, because the emission from the inner region of the dust torus irradiated by the AGN is dominant in the NIR waveband. This is supported by the thermal dust reverberation measurements on NGC4151 (Minezaki et al. 2004). In Fig. 1, we plot the relation between the ratios $L_{\text{bol}}/L_{\text{Edd}}$ and $L_{\text{NIR}}/L_{\text{bol}}$. No correlation is found between these two ratios.

Haas et al. (2003) suggested a scheme of quasar evolution for their dust distribution surrounding the AGNs. The sources are divided into different classes according to their evolutionary sequence. The classes 0 and 1 represent cool and warm

ultra-luminous infrared galaxies respectively. Class 2 sources are young quasars, and the starbursts are still important in IR wavebands compared with the torus emission. There are two class 2 quasars in this sample, and we leave out these two infrared luminous quasars 0157+001 and 1351+640 in all our statistic analysis, because the contribution in the infrared waveband by the dust heated by the stars in these two quasars may not be neglected, though these two sources would only affect little on the statistic results. The relation between the black hole mass M_{bh} and the ratio $L_{\text{NIR}}/L_{\text{bol}}$ is plotted in Fig. 2. The generalized Kendall's τ test (Astronomical Survival Analysis, ASURV, Feigelson & Nelson 1985) shows that the correlation is significant at the 99.93 per cent level for the whole sample of 52 sources (the significant level is almost same at the 99.94 per cent for the sample of 42 BL quasars). The linear regression by parametric expectation-maximization (EM) Algorithm (ASURV) gives

$$\log_{10} L_{\text{NIR}}/L_{\text{bol}} = -0.097(\pm 0.034) \log_{10} M_{\text{bh}}/M_{\odot} - 0.125(\pm 0.279), \quad (12)$$

for the whole sample (the solid line in Fig. 2), and

$$\log_{10} L_{\text{NIR}}/L_{\text{bol}} = -0.149(\pm 0.038) \log_{10} M_{\text{bh}}/M_{\odot} + 0.325(\pm 0.322), \quad (13)$$

for the broad-line quasars (the dotted line in Fig. 2), respectively. Compared with the linear regression for the whole sample, the slope becomes slightly steeper for the BL quasars, while the correlation levels are almost same. For those 13 radio-loud quasars in this sample, no statistic behavior systematically different from the radio-quiet quasars is found.

The BLR size R_{BLR} is derived from the optical continuum luminosity at 5100 Å, so the estimated black hole mass $M_{\text{bh}} \propto v_{\text{BLR}}^2 L_{\lambda}^{0.61}(5100)$ is given by substituting Eq. (1) into Eq. (2). The bolometric luminosity L_{bol} is estimated from the optical continuum luminosity by using the empirical relation (3). It is therefore doubtful that the correlation between the black hole mass M_{bh} and the ratio $L_{\text{NIR}}/L_{\text{bol}}$ may be caused by the common dependence of optical continuum luminosity L_{λ} . We plot the relation between the bolometric luminosity L_{bol} and the ratio $L_{\text{NIR}}/L_{\text{bol}}$ in Fig. 3. It is found that the bolometric luminosity L_{bol} is correlated with the ratio $L_{\text{NIR}}/L_{\text{bol}}$ for the whole sample. In order to test the correlation between the black hole mass M_{bh} and the ratio $L_{\text{NIR}}/L_{\text{bol}}$ is affected to what extent by the common dependence of the optical continuum luminosity, we perform statistic analysis on the sources with $10^{45} \text{ erg s}^{-1} \leq L_{\text{bol}} \leq 10^{46.5} \text{ erg s}^{-1}$ (35 sources situated between the two dotted lines in Fig. 3). We find that the ratio $L_{\text{NIR}}/L_{\text{bol}}$ is still significantly correlated with the black hole mass M_{bh} at the 97.25 per cent level for this sub-sample of 35 quasars, while no correlation is found between L_{bol} and $L_{\text{NIR}}/L_{\text{bol}}$ (at the 75.01 per cent level). This means that the ratio $L_{\text{NIR}}/L_{\text{bol}}$ is intrinsically correlated with the black hole mass M_{bh} .

We also perform statistic analysis on the relations: $M_{\text{bh}} - L_{\text{MIR}}/L_{\text{bol}}$, $M_{\text{bh}} - L_{\text{FIR}}/L_{\text{bol}}$, and $M_{\text{bh}} - L_{\text{IR}}/L_{\text{bol}}$ (see Figs. 4-6). The mid-infrared (MIR, 10–40 μm), far-infrared (FIR, 40–150 μm), and total infrared (IR, 3–150 μm) luminosities of these quasars are taken from Haas et al. (2003). It is found that they are significantly correlated at the similar levels as the NIR case, while the slope becomes steeper for the FIR case. There are three sources in our sample have $L_{\text{IR}}/L_{\text{bol}} \gtrsim 1$ (see Fig. 6). The detailed statistic results are summarized in Table 1.

The dust clouds at the inner radius R_{in} of the torus irradiated by the AGN emit mostly in the NIR waveband. The

covering factor f_{in} at R_{in} can be estimated by using the relation (8). Subtracting the three sources with $L_{\text{IR}}/L_{\text{bol}} \gtrsim 1$ and the infrared luminous source 1351+640, we find that the ratios $L_{\text{NIR}}/L_{\text{IR}}$ for the sources in our present sample are in the range 0.20–0.56 with an average of 0.39. We use Eq. (11) to estimate the torus thickness at its inner radius R_{in} adopting a covering factor $f_{\text{in}} = 0.39$. The relations of $M_{\text{bh}} - H(R_{\text{in}})$ and $L_{\text{bol}} - H(R_{\text{in}})$ are plotted in Figs. 7 and 8 respectively. It is found that the torus thickness H at its inner radius R_{in} increases with the black hole mass M_{bh} and the bolometric luminosity L_{bol} .

The solid angle $\Delta\Omega_{\text{torus}}$ subtended by the whole torus can be estimated by using Eq. (7) from the ratio $L_{\text{IR}}/L_{\text{bol}}$. We can then calculate the relative torus thickness H/R using Eq. (9). In Fig. 9, we plot the relation between the black hole mass M_{bh} and the relative torus thickness H/R . The three sources with $L_{\text{IR}}/L_{\text{bol}} \gtrsim 1$ do not appear in this figure. The statistic results are listed in Table 1.

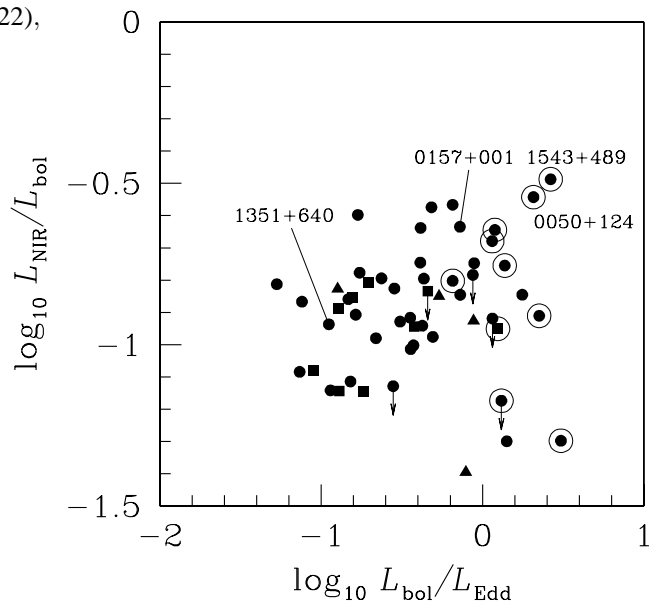


FIG. 1.— The relation between the ratios $L_{\text{bol}}/L_{\text{Edd}}$ and $L_{\text{NIR}}/L_{\text{bol}}$. The circles represent radio-quiet quasars, while the squares and triangles represent steep-spectrum and flat-spectrum radio quasars, respectively. The sources with large circles have $\text{FWHM}(H\beta) < 2000 \text{ km s}^{-1}$. The relation between the ratios $L_{\text{bol}}/L_{\text{Edd}}$ and $L_{\text{NIR}}/L_{\text{bol}}$.

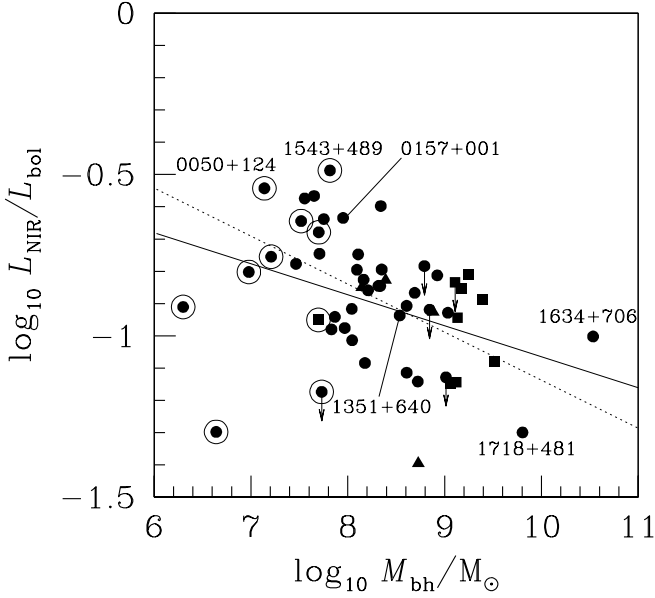


FIG. 2.— The relation between the black hole mass M_{bh} and the ratio $L_{\text{NIR}}/L_{\text{bol}}$. The solid line represents the linear regression for the whole sample but excluding two infrared luminous sources 0157+001 and 1351+640. The dotted line represents the linear regression for the sources with $\text{FWHM}(\text{H}\beta) \geq 2000 \text{ km s}^{-1}$ excluding two sources 0157+001 and 1351+640.

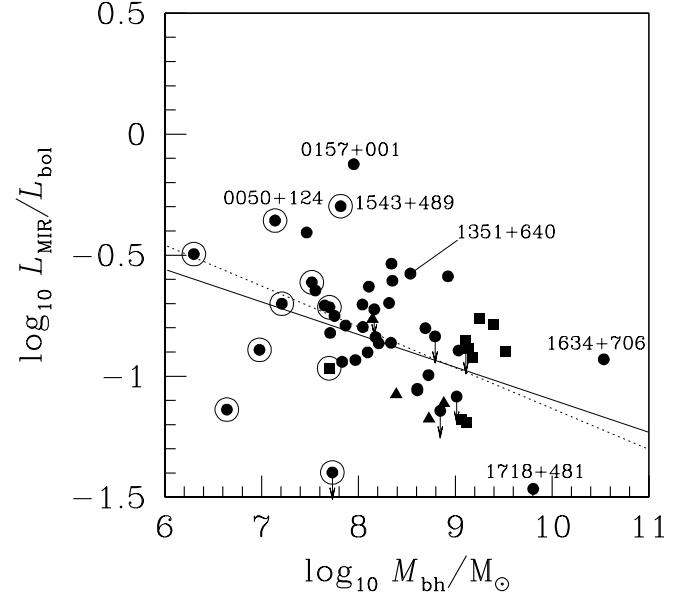


FIG. 4.— Same as Fig. 2, but for the ratio $L_{\text{MIR}}/L_{\text{bol}}$.

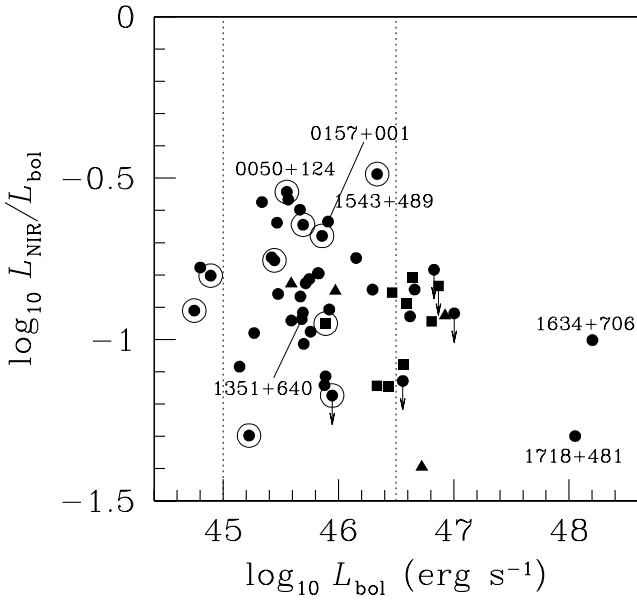


FIG. 3.— The relation between the ratios L_{bol} and $L_{\text{NIR}}/L_{\text{bol}}$. The dotted lines represent $L_{\text{bol}} = 10^{45} \text{ erg s}^{-1}$ and $10^{46.5} \text{ erg s}^{-1}$.

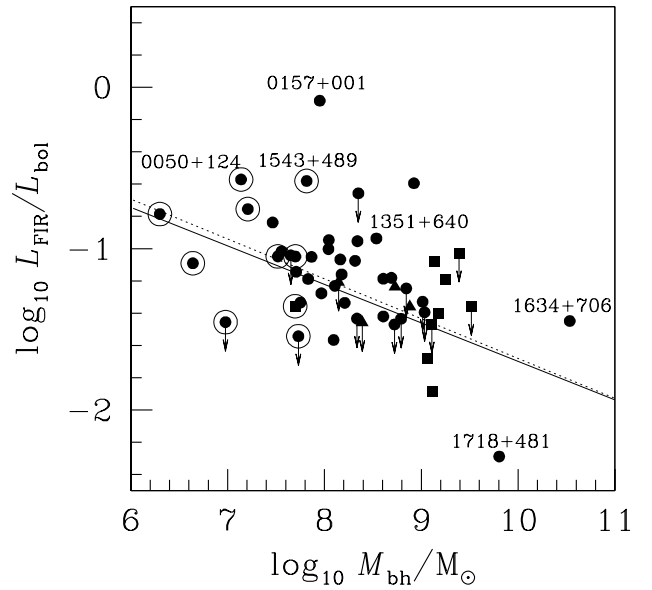


FIG. 5.— Same as Fig. 2, but for the ratio $L_{\text{FIR}}/L_{\text{bol}}$.

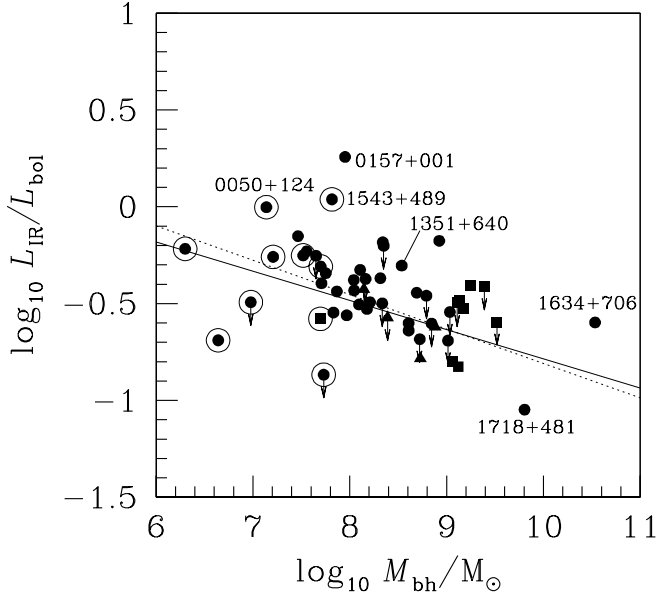


FIG. 6.— Same as Fig. 2, but for the ratio $L_{\text{IR}}(3-150\mu\text{m})/L_{\text{bol}}$.

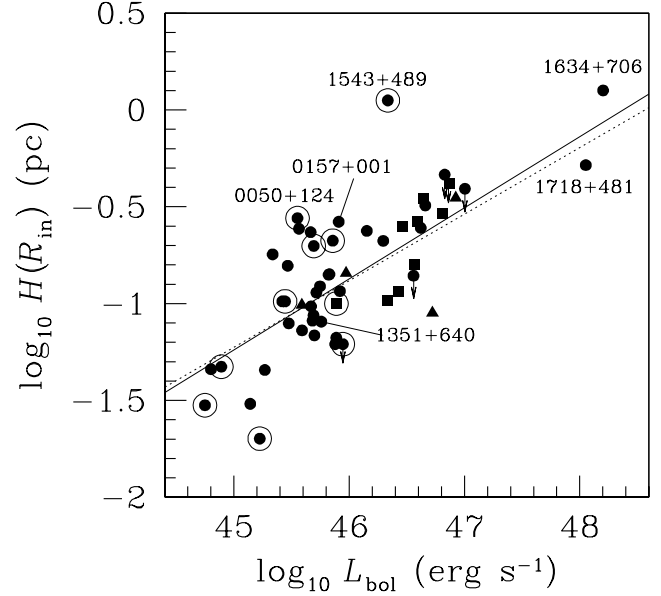


FIG. 8.— The relation between the bolometric luminosity L_{bol} and the torus thickness $H(R_{\text{in}})$ at its inner radius R_{in} . The solid line represents the linear regression for the whole sample but excluding the infrared luminous sources 0157+001 and 1351+640. The dotted line represents the linear regression for the sources with $\text{FWHM}(\text{H}\beta) \geq 2000 \text{ km s}^{-1}$ excluding the sources 0157+001 and 1351+640.

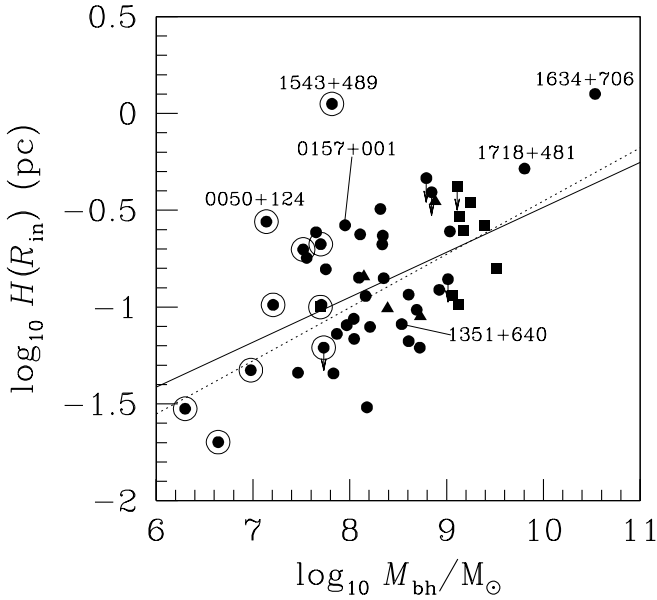


FIG. 7.— The relation between the black hole mass M_{bh} and the torus thickness $H(R_{\text{in}})$ at its inner radius R_{in} . The solid line represents the linear regression for the whole sample but excluding the infrared luminous sources 0157+001 and 1351+640. The dotted line represents the linear regression for the sources with $\text{FWHM}(\text{H}\beta) \geq 2000 \text{ km s}^{-1}$ excluding the sources 0157+001 and 1351+640.

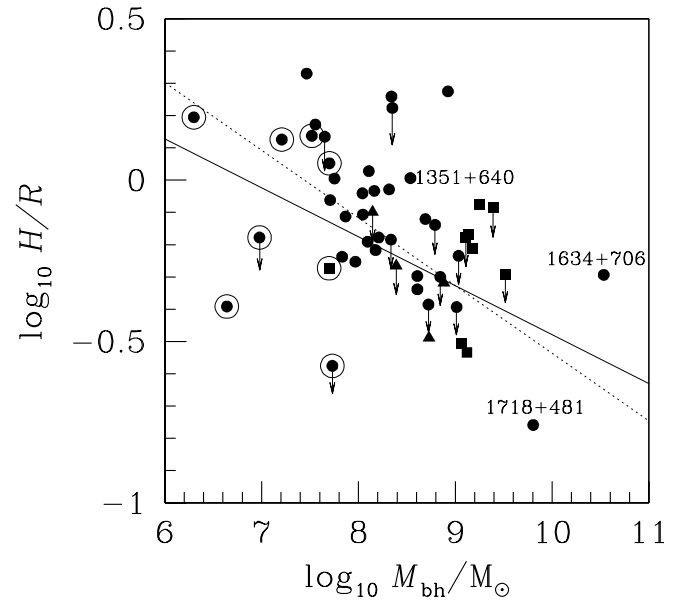


FIG. 9.— The relation between black hole mass M_{bh} and the relative thickness of the torus H/R .

6. DISCUSSION

The NIR luminosities L_{NIR} of the PG quasars in the waveband of $3-10 \mu\text{m}$ given by Haas et al. (2003) are used in this work. The NIR emission in the waveband $\gtrsim 2 \mu\text{m}$ is dominated by the thermal emission from the dust torus, which is supported by the decomposition of the SEDs of the Seyfert galaxies and the thermal dust reverberation measurements on NGC4151 (Kobayashi et al. 1993; Minezaki et al. 2004). The NIR emission $\sim 2 \mu\text{m}$ is not included in the NIR luminosities L_{NIR} provided by Haas et al. (2003), so the solid angle Ω_{torus} subtended by the torus may be slightly larger than that estimated from the ratio $L_{\text{NIR}}/L_{\text{bol}}$ by using the relation (6). No correlation is found between the ratios $L_{\text{bol}}/L_{\text{Edd}}$ and $L_{\text{NIR}}/L_{\text{bol}}$, which implies that the solid angle $\Delta\Omega_{\text{torus}}$ subtended by the dust torus does not evolve with the accretion rate \dot{m} . In the clumpy dust cloud model (Krolik & Begelman 1988), the dimensionless torus thickness is estimated by

$$\frac{H}{R} \sim \frac{2V_c}{V_K}, \quad (14)$$

where V_c is the typical random velocity of the dust clouds and V_K is the Keplerian velocity at radius R . This means the ratio of the typical dust cloud random velocity to the Keplerian velocity V_c/V_K is independent of the dimensionless accretion rate \dot{m} . However, it should be cautious that the PG quasars are optically selected and they are very bright (most sources have $L_{\text{bol}}/L_{\text{Edd}} \gtrsim 0.1$, see Fig. 1). We cannot rule out the presence of a correlation between the ratios $L_{\text{bol}}/L_{\text{Edd}}$ and $L_{\text{NIR}}/L_{\text{bol}}$, if more fainter quasars with lower values of $L_{\text{bol}}/L_{\text{Edd}}$ are included in the statistic analysis.

The intrinsic correlation between black hole mass M_{bh} and the ratio $L_{\text{NIR}}/L_{\text{bol}}$ indicates that the dust torus geometry is related with the central black hole mass. The larger black hole leads to a dust torus with smaller solid angle subtended by it seen from the central source. The black hole grows slowly during its bright quasar phase (usually less than a factor of 2, see Kauffmann & Haehnelt, 2000), because the typical timescale for the bright quasar phase is $\sim 10^{7-8}$ years (e.g., Yu & Tremaine, 2002). This means that the black hole mass estimated from the broad-line width and the optical continuum luminosity can roughly reflect the hole mass while the bright quasar was formed at an early time. If the dust torus was formed at nearly the same time as the bright quasar, it may imply that the formation of the dust torus is regulated by the central black hole, though the detailed mechanism is still unclear. Zier & Biermann (2001, 2002) suggested a torus formation scenario that the merger of binary black holes may lead the distribution of the surrounding matter to be a torus-like structure. In this scenario, the black holes play important roles in the formation of the torus, which is in general consistent with our statistic results.

Similar correlations between the black hole mass M_{bh} and the ratio $L_{\text{IR}}/L_{\text{bol}}$ are also found for the MIR and FIR cases (see Fig. 4 and 5). This implies that the emission in the MIR and FIR wavebands is dominated by the thermal dust tori heated by the central AGNs, excepting the infrared luminous quasars 0157+001. This source has very high ratios of the infrared to bolometric luminosities, especially in the MIR and FIR wavebands, which implies that the starbursts in this source contribute much in the MIR and FIR wavebands than the NIR waveband. It is still unclear why the slope of the correlation between M_{bh} and $L_{\text{FIR}}/L_{\text{bol}}$ is steeper than that for the NIR and MIR cases (see Table 1 for comparison). One likely explanation is that the torus properties (e.g., number of

the clouds and their distribution, and the cloud optical depth, etc.) or/and the AGN spectral shape vary systematically with the black hole mass M_{bh} , because the spectrum emitted from the dust torus is determined by the torus properties, and the SED of the AGN (e.g., Nenkova, Ivezić, & Elitzur, 2002). The detailed model calculations, for example, with the code DUSTY (Nenkova, Ivezić, & Elitzur 2002), are necessary for solving this issue, which are beyond the scope of this work. An alternative explanation is that the starbursts contribution in the FIR waveband is more important than the NIR and MIR wavebands, and the thermal emission from the dust torus irradiated by the AGN contributes less in the FIR waveband. In this case, the starbursts contribution is supposed to change the slope of the correlation between M_{bh} and $L_{\text{FIR}}/L_{\text{bol}}$, while it should still not be dominant to avoid destroying this correlation. This can be explained by recent IR observations showing that the nuclear starbursts are in the dusty tori around the nuclei of some Seyfert galaxies (Imanishi & Wada 2004).

For most quasars in our sample, the IR emission is dominantly from the tori irradiated by the AGNs. In this case, the IR luminosity should be less than the bolometric luminosity. In Fig. 6, we find three sources with $L_{\text{IR}}(3-150 \mu\text{m})/L_{\text{bol}} \gtrsim 1$. The IR emission from these four sources (including one class 2 quasars: 0157+001; two narrow-line quasars: 0050+124 and 1543+489) cannot be solely produced by the dust torus heated by the AGNs. The contribution of stars in the host galaxies should be important in these four quasars. The ratio $L_{\text{IR}}/L_{\text{bol}} \gtrsim 1$ can therefore be used as a criterion for starbursts dominant quasars. The detailed geometry of the dust torus is still unclear. The opening angle of the torus may vary with radius. However, the ratio $L_{\text{IR}}/L_{\text{bol}}$ can always be used to estimate the solid angle subtended by the whole torus. For those four quasars with $L_{\text{IR}}/L_{\text{bol}} > 1$, the IR emission is dominated by the starbursts and we are not able to estimate the solid angle subtended by the torus from the ratio $L_{\text{IR}}/L_{\text{bol}}$. We find that the relative torus thickness H/R estimated from the ratio $L_{\text{IR}}/L_{\text{bol}}$ is in the range of 0.2–2.4 with an average of ~ 0.9 (see Fig. 9). This is different from $H/R \sim 2-3$ estimated from the fraction of quasars in the 3CR sample (Hill, Goodrich, & Depoy 1996).

We may estimate the solid angle $\Delta\Omega_{\text{torus}}$ subtended by the torus at its inner radius from the ratio of the NIR to bolometric luminosities, because the NIR emission is dominated by the emission from the dust clouds at its inner radius irradiated by the AGN. The emission in the NIR waveband is less affected by the starbursts compared with the MIR and FIR wavebands. If the opening angle is constant for the torus at different radius, the covering factor of the clouds at the inner radius can be estimated from the ratio $L_{\text{NIR}}/L_{\text{IR}}$ (Eq. 8). It implies that only a fraction of the nuclear radiation is absorbed by the dust clouds at the inner radius of the torus. The remainder may be absorbed by the dust clouds at larger radii, and they have lower temperatures than that at the inner radius. Most of their emission may be in the MIR or FIR wavebands depending on their distance from the nucleus. This is consistent with the fact that similar correlations are found between M_{bh} and $L_{\text{IR}}/L_{\text{bol}}$ for the MIR and FIR cases. We use a constant covering factor $f_{\text{in}} = 0.39$ to estimate the torus thickness $H(R_{\text{in}})$ at its inner radius. The slope of the correlation between $M_{\text{bh}} - H(R_{\text{in}})$ is ~ 0.23 (see Table 1), which is obviously non-linear. The correlation between L_{bol} and $H(R_{\text{in}})$ has a slope of ~ 0.37 , which is different from the constant torus thickness H with luminosity assumed in the receding torus model suggested by Hill, Goodrich, & Depoy (1996). The further IR observations

TABLE 1
RESULTS OF STATISTIC ANALYSIS

| Relation | Sample | Significant level (per cent) | a | b |
|---|----------------|------------------------------|--------------------|---------------------|
| $M_{\text{bh}} - L_{\text{NIR}}/L_{\text{bol}}$ | All | 99.93 | -0.097 ± 0.034 | -0.125 ± 0.279 |
| | BL quasars | 99.94 | -0.149 ± 0.038 | 0.325 ± 0.322 |
| $M_{\text{bh}} - L_{\text{MIR}}/L_{\text{bol}}$ | All | 99.94 | -0.135 ± 0.040 | 0.224 ± 0.335 |
| | BL quasars | 99.85 | -0.169 ± 0.045 | 0.526 ± 0.381 |
| $M_{\text{bh}} - L_{\text{FIR}}/L_{\text{bol}}$ | All | 99.99 | -0.239 ± 0.058 | 0.658 ± 0.475 |
| | BL quasars | 99.88 | -0.255 ± 0.073 | 0.809 ± 0.625 |
| $M_{\text{bh}} - L_{\text{IR}}/L_{\text{bol}}$ | All | 99.98 | -0.151 ± 0.040 | 0.697 ± 0.330 |
| | BL quasars | 99.93 | -0.178 ± 0.044 | 0.941 ± 0.376 |
| $M_{\text{bh}} - H_{\text{in}}$ | All | 99.51 | 0.232 ± 0.054 | -2.825 ± 0.452 |
| | BL quasars | 99.51 | 0.275 ± 0.061 | -3.220 ± 0.523 |
| $L_{\text{bol}} - H_{\text{in}}$ | All | > 99.99 | 0.367 ± 0.051 | -17.760 ± 2.320 |
| | BL quasars | > 99.99 | 0.344 ± 0.044 | -16.708 ± 2.019 |
| $M_{\text{bh}} - H/R$ | All(50) | 99.93 | -0.152 ± 0.045 | 1.011 ± 0.376 |
| | BL quasars(42) | 99.93 | -0.210 ± 0.054 | 1.532 ± 0.461 |

NOTE. — Columns (3) and (4): coefficients of the linear regression: $\log_{10} Y = a \log_{10} X + b$.

on a larger quasar sample including more fainter quasars by the Spitzer Space Telescope will help understand the physics of the dust tori in quasars.

I am grateful to X.Y. Xia for stimulating discussion, and C. Zier for his helpful explanation of their torus formation model. I thank Caina Hao for pointing me an error in the original manuscript. This work is supported by the Na-

tional Science Fund for Distinguished Young Scholars (grant 10325314), NSFC (grants 10173016; 10333020), and the NKBRSF (grant G1999075403). This research has made use of the NASA/IPAC Extragalactic Database (NED), which is operated by the Jet Propulsion Laboratory, California Institute of Technology, under contract with the National Aeronautic and Space Administration.

REFERENCES

- Antonucci, R., 1993, *ARA&A*, 31, 473
Antonucci, R., & Miller, J.S., 1985, *ApJ*, 297, 621
Barthel, P.D., 1989, *ApJ*, 336, 606
Boroson T.A., Green, R.F., 1992, *ApJS*, 80, 109
Brotherton, M.S., 1996, *ApJS*, 102, 1
Cao, X., & Jiang, D.R., 2002, *MNRAS*, 331, 111
Feigelson E.D., & Nelson P.I., 1985, *ApJ*, 293, 192
Haas, M., et al., 2003, *A&A*, 402, 87
Hill, G.J., Goodrich, R.W., & Depoy, D.L., 1996, *ApJ*, 462, 163
Imanishi, M., & Wada, K., 2004, *ApJ*, in press, astro-ph/0408422
Kaspi S., Smith P.S., Netzer H., Maoz D., Jannuzi B.T., & Giveon U., 2000, *ApJ*, 533, 631
Kauffmann, G., & Haehnelt, M., 2000, *MNRAS*, 311, 576
Kobayashi, Y., Sato, S., Yamashita, T., Shiba, H., & Takami, H., 1993, *ApJ*, 404, 94
Krolik, J.H., & Begelman, M.C., 1988, *ApJ*, 329, 702
Lawrence, A., 1991, *MNRAS*, 252, 586
McLure, R.J., & Jarvis, M.J., 2002, *MNRAS*, 337, 109
Miller, J.S., & Goodrich, R.W., 1990, *ApJ*, 355, 456
Minezaki, T., Yoshii, Y., Kobayashi, Y., Enya, K., Suganuma, M., Tomita, H., Aoki, T., & Peterson, B., 2004, *ApJ*, 600, L35
Nenkova, M., Ivezić, Z., & Elitzur, M., 2002, *ApJ*, 570, L9
Netzer, H., & Laor, A., 1993, *ApJ*, 404, L51
Peterson, B. M., 1993, *PASP*, 105, 247
Shields, G.A., Gebhardt, K., Salviander, S., Wills, B.J., Xie, B., Brotherton, M.S., Yuan, J., & Dietrich, M., 2003, *ApJ*, 583, 124
Tran, H.D., 1995, *ApJ*, 440, 597
Yu, Q., & Tremaine, S., 2002, *MNRAS*, 335, 965
Zier, C., & Biermann, P.L., 2001, *A&A*, 377, 23
Zier, C., & Biermann, P.L., 2002, *A&A*, 396, 91